Summertime Precipitation Variability over Europe and its Links to Atmospheric Dynamics and Evaporation

Igor I. Zveryaev and Richard P. Allan*

P.P. Shirshov Institute of Oceanology, RAS, Moscow, Russia

*Environmental Systems Science Centre, University of Reading, Reading, UK

Revised version submitted to JGR-Atmospheres

November, 2009

Address for correspondence:

Dr. Igor I. Zveryaev, P.P. Shirshov Institute of Oceanology, RAS

36, Nakhimovsky Ave., Moscow, 117997, Russia

Telephone: 7 (495) 1247928

Telefax: 7 (495) 1245983

Email: igorz@sail.msk.ru

Abstract

Gridded monthly precipitation data for 1979-2006 from the Global Precipitation Climatology Project (GPCP) are used to investigate interannual summer precipitation variability over Europe and its links to regional atmospheric circulation and evaporation.

The first EOF mode of European precipitation, explaining 17.2-22.8% of its total variance, is stable during the summer season and is associated with the North Atlantic Oscillation (NAO). The spatial-temporal structure of the second EOF mode is less stable and shows month-to-month variations during the summer season. This mode is linked to the Scandinavian teleconnection pattern.

Analysis of links between leading EOF modes of regional precipitation and evaporation has revealed a significant link between precipitation and evaporation from the European land surface, thus indicating an important role of the local processes in summertime precipitation variability over Europe. Weaker, but statistically significant links have been found for evaporation from the surface of the Mediterranean and Baltic Seas. Finally, in contrast to winter, no significant links have been revealed between European precipitation and evaporation in the North Atlantic during the summer season.

1. Introduction

Variability of precipitation in the European region on a variety of time-scales substantially impacts human activities. Climate anomalies associated with deficient/excessive precipitation may lead to serious social and economic consequences. Recently, there were several examples of such climate anomalies in different parts of Europe that resulted in significant damage to regional economies [e.g., *Christensen and Christensen,* 2003; *Schär et al.,* 2004; *Marsh and Hannaford,* 2007; *Blackburn et al.,* 2008, *Lenderink et al.,* 2009]. Many regional climate extremes occur during summer. One of the most recent examples of such extremes is the anomalously high precipitation over Great Britain during summer 2007 and this resulted in extensive flooding across England and Wales [*Marsh and Hannaford,* 2007; *Blackburn et al.,* 2008]. Nevertheless, compared to winter, significantly less attention has been given to analysis of the European climate variability during the summer season [e.g., *Colman and Davey*, 1999; *Hurrell and Folland,* 2002; *Zveryaev,* 2004; Zolina et al., 2008]. In general, summertime climate variability in the European region is not well studied or understood. Moreover, predictability of the climate in mid-latitudes for the summer season shows generally lower skill than that for the winter season [e.g., *Colman and Davey,* 1999; *Dirmeyer et al.,* 2003; *Koenigk and Mikolajewicz,* 2008]. In particular, based on analysis of the North Atlantic sea surface temperature anomalies, *Colman and Davey* [1999] found quite low skills of statistical predictability of European climate during summer. Therefore, to improve prediction of regional climate and its extremes, particularly for the warm season, further analysis of the processes driving European climate variability is necessary.

In contrast to winter, when European precipitation variability is mostly driven by the North Atlantic Oscillation [NAO, e.g., *Hurrell,* 1995; *Qian et al.,* 2000; *Zveryaev,* 2006], mechanisms driving interannual variability of regional precipitation during summer are more complex and are not well understood. In summer, when the role of atmospheric moisture advection in precipitation variability is diminished, the role of the local land surface processes increases [*Trenberth,* 1999]. Some studies point to the importance of land surface processes in summer precipitation variability [*Koster and Suarez,* 1995; *Schär et al.,* 1999; *Seneviratne et al.,* 2006], whereas other works highlight the role of the summer atmospheric circulation [*Pal et al.,* 2004; *Koster et al.,* 2004; *Ogi et al.,* 2005]. Although the above mechanisms are not mutually exclusive, there is a high degree of uncertainty regarding their role in summer precipitation variability in the Northern Hemisphere extra-tropics, and particularly over Europe.

The present study focuses on the analysis of the summer precipitation variability over Europe on an interannual time scale, and on the links between this variability and regimes of the atmospheric circulation in the Atlantic-European sector. While our recent studies [*Zveryaev,* 2004; 2006] highlighted seasonal differences in precipitation variability over Europe and were based on analysis of seasonal mean precipitation, the present study examines summer season evolution of the leading modes of regional precipitation. In other words, we address the question of how stable are the leading modes of summer season precipitation, a highly variable (both in time and space) climate parameter. We also examine stability of the links between the leading modes of regional precipitation and regimes of atmospheric circulation during summer season. Note, our recent analysis [*Zveryaev,* 2006; 2009] revealed significant interdecadal changes in such links. Furthermore, we investigate connection between European precipitation and evaporation from the surface of the North Atlantic Ocean, the Mediterranean and Baltic Seas, and from the European land surface. We analyze variability of precipitation over Europe on the basis of data available from the Global Precipitation Climatology Project (GPCP) dataset for

1979-2006 [*Huffman et al.,* 1997; *Adler et al.,* 2003]. In order to get more detailed information on the summer precipitation variability and to examine stability of the leading modes of precipitation during the summer season, we performed analysis for summer seasonal mean precipitation as well as separate analyses for each summer month. The paper is organized as follows. The data used and the analysis methods are described in section 2. Spatial-temporal structure of the leading modes of the summer seasonal and monthly mean precipitation variability for 1979-2006 and their links to regional atmospheric circulation are analyzed in section 3. In section 4 we explore links between regional precipitation and evaporation during summer season. Finally, summary and discussion are presented in section 5.

2. Data and methods

We employed monthly mean global precipitation data (2.5° x 2.5° latitude-longitude grid) from the Version-2 of the GPCP dataset for 1979-2006 [*Huffman et al.,* 1997; *Adler et al.,* 2003]. The GPCP data set represents a combination of gauge observations and satellite estimates. There were several reasons to choose this dataset. First (and most important), since the European climate experiences significant interdecadal and longer trend-like changes, in the present study we were interested in characterizing interannual variability during the most recent climate period, thought to be the warmest since the beginning of instrumental observations [e.g., *Trenberth et al.,* 2007]. Permanently updated GPCP data provides more up-to-date information compared to the Climatic Research Unit (CRU) dataset [*New et al.,* 1999; *Mitchell and Jones,* 2005] which has finer spatial resolution, but is not so regularly updated. Moreover, it was shown that for the European region there is reasonably good agreement between satellite-based precipitation products and the CRU dataset [e.g., *Zveryaev,* 2004]. Note the data quality over oceanic/marine regions in the GPCP dataset is somewhat lower (compared to the land areas) since it is based exclusively on satellite estimates. In the present study the domain of analysis is limited to latitudes 30°N-75°N and longitudes 15°W-52.5°E.

In this study we also used evaporation data from the Woods Hole Oceanographic Institution (WHOI) data set [*Yu and Weller,* 2007]. In contrast to other flux products constructed from one single data source, this data set is determined by objectively blending the data sources from satellite and NWP model outputs while using in situ observations to assign the weights [*Yu et al.,* 2004; *Yu and Weller,* 2007]. The WHOI data set provides evaporation data (1° x 1° latitude-longitude grid) over the global oceans for 1958-2006. Detailed description of the data and the synthesis procedure can be found in *Yu and Weller* [2007] and at the website http://oaflux.whoi.edu. Since observational data over land are rather scarce, as a complementary data source on evaporation over the land surface we used data from the NCEP/NCAR Reanalysis for 1979-2006 [*Kalnay et al.,* 1996]. These data are diagnostic outputs from 6-hourly forecasts produced by a numerical weather prediction model in data assimilation mode. Since evaporation is not directly assimilated, model bias may influence the reliability of these fields, thereby limiting the accuracy in representing links between aspects of the regional water cycle. It is recognized that the quality of precipitation data in reanalyses is poor [e.g., *Zolina et al.,* 2004]. Since precipitation influences soil moisture and land surface evaporation, the quality of evaporation in reanalyses is also questionable. It should be stressed that there is a relaxation to a seasonal climatology term in the reanalysis surface water equation [e.g., *Roads et al.,* 1999]. The reason for this artificial source of water is that preliminary experiments showed that the reanalysis surface water would have drifted and would have negatively impacted other near-surface and atmospheric variables, in particular, precipitation. Thus, the reanalysis is being forced toward climatology that is somewhat inconsistent with its land surface parameterization. We nevertheless hope to obtain reasonable qualitative assessments of these links within the degree of uncertainty provided by the reanalysis product.

To assess the links between variability of European precipitation and regional atmospheric circulation we use indices of the major teleconnection patterns that have been documented and described by *Barnston and Livezey* [1987]. In our analysis along with links to the NAO we examine links to such teleconnections as the East Atlantic (EA) pattern, East Atlantic – West Russia (EAWR) pattern, and Scandinavian (SCA) pattern, which can also affect European precipitation variability. The data cover the period 1950 - present. Details on the teleconnection pattern calculation procedures can be found in *Barnston and Livezey* [1987] and at the CPC website. To reveal the dynamical context of the leading modes in precipitation variability, we used monthly sea level pressure (SLP) and 500hPa heights data from the NCEP/NCAR Reanalysis for 1979-2006 [*Kalnay et al.,* 1996].

We examine the spatial-temporal structure of long-term variations in summer monthly and seasonal mean precipitation over Europe by application of conventional empirical orthogonal functions (EOF) analysis [*Wilks*, 1995; *von Storch and Navarra,* 1995]. To assess links to teleconnections we used standard correlation analysis. It should be emphasized that statistical methods used imply that only linear relationships between different climate variables (and mechanisms forming them) in European region are addressed in this study.

3. Leading modes of the summer precipitation over Europe and their links to atmospheric dynamics.

To reveal the leading modes of interannual variability of precipitation over Europe during summer, we performed the EOF analysis on time series of the summer (June-July-August) mean and (separately) June, July and August monthly mean precipitation from the GPCP data set for the period 1979 – 2006. The time series were linearly detrended and anomalies were weighted by the square root of cosine of latitude [*North et al.,* 1982]. As we earlier mentioned, the motivation for the separate analyses of the monthly precipitation time series is based on our intention to examine the stability of the leading EOF modes during the summer season. We limit our analysis to consideration of the first two EOF modes, because each of the subsequent modes explains less than 10% of the total precipitation variance, and because significant links between those modes of precipitation variability and regimes of atmospheric circulation have not been revealed. It should be noted that in August the leading EOF modes of precipitation are not well separated according to the North criteria [*North et al.,* 1982], however, we include them into our consideration for the sake of completeness of analysis. Spatial patterns of the first two EOF modes of precipitation and time series of the corresponding principal components (hereafter PC) are shown, respectively, in Figures 1 and 2.

The first EOF mode explains from 17.2% (in June) to 22.8% (in July) of the total variance of precipitation. The respective spatial patterns (Figure 1a, c, e, g), characterized by a tripole-like structure, depict three action centers. The major action center extends from the British Isles to a wide region around the Baltic Sea, and further to eastern Europe and European Russia. Two other centers of opposite polarity are located to the south (i.e. over Mediterranean region) and north (i.e. over northern Scandinavia) of the major action center (Figure 1a, c, e, g). Structurally the obtained patterns are very similar to that of the first EOF mode of the mean summer precipitation from the CMAP data for 1979-2001 [*Zveryaev,* 2004]. We note that the structure of the EOF-1 patterns demonstrates evident persistence during the summer season. In other words, structural changes from month to month are not significant, albeit local (i.e. in action centers) changes in magnitudes of variability are noticeable. It is worth noting that *Casty et al.* [2007] obtained a similar pattern from analysis of a longer (1766-2000) time series of summer seasonal mean precipitation over Europe. The PC-1 (Figure 2a, c, e, g), displaying temporal behavior of this mode, demonstrates evident correspondence with the NAO index in all considered months and in analysis of seasonal mean precipitation. Moreover, high (and statistically significant according to the Student's *t*-test [*Bendat and Piersol,* 1966]) correlations between respective PCs and the NAO index (Table 1) clearly indicate that during the entire summer season EOF-1 of European precipitation is associated with the NAO. It should be noted, however, that summer NAO is essentially different (in terms of its spatial structure) from its winter counterpart [*Barnston and Livezey,* 1987]. In particular, location of the summer NAO action centers is quite different [*Wanner et al.,* 1997; *Mächel et al.,* 1998; *Portis et al.,* 2001]. Hence, the NAO-associated summer precipitation patterns (Figure 1a, c, e, g) are also principally different from the winter dipole-like patterns [e.g., *Hurrell,* 1995; *Zveryaev,* 2004].

The second EOF mode of summer precipitation over Europe accounts for 12.4-15.3% of its total variance. The spatial pattern of this mode (Figure 1b, d, f, h) in general represents a meridional dipole characterized by the coherent precipitation variations over the northern part of European Russia and Scandinavia and opposite variations over the remaining part of Europe. In particular, the pattern is well depicted in July (Figure 1f). However, in contrast to the first EOF, there are evident month-to-month changes in the structure of the second EOF mode. For example, in June (Figure 1d) the largest loadings are observed over western Europe and western Scandinavia, whereas in July (Figure 1f) they are revealed over eastern Europe and European

Russia. In August (Figure 1h) the entire dipole demonstrates zonal rather than meridional orientation. Therefore, the second EOF mode of precipitation is less stable during the summer season compared to the first mode. Figures 2d, f, h and results of correlation analysis (Table 1) imply that this mode of European precipitation is driven mainly by the SCA teleconnection pattern [*Barnston and Livezey,* 1987], consisting of the major action center over Scandinavia, and minor action centers of opposite polarity over western Europe and eastern Russia. Note, however, the second EOF mode of summer mean precipitation does not demonstrate a significant link to the mean summer SCA index. A possible reason for this is that the mean summer SCA index is defined not as a respective EOF mode obtained from analysis of summer mean 500hPa geopotential heights (CPC does not provide such seasonal indices), but as the average from the SCA indices estimated for June, July and August. Since interannual behavior of these monthly indices is rather different (Figures 2d, f, h), their average can hardly be viewed as a representative parameter reflecting interannual variability of summer mean atmospheric circulation.

We further briefly analyze the leading EOF modes of the SLP and 500hPa fields in Atlantic-European sector and their links to European precipitation. Since there is general consistency between leading EOF modes of precipitation (and other considered climate variables) estimated for different summer months (and for the seasonal mean), and in order to avoid repetition, we show relevant figures only for July (central summer month). It should be stressed, however, that further analysis in this and next section was performed for each summer month.

The spatial patterns of the EOF-1 of July 500hPa heights and SLP (Figures 3a, c) represent the summer NAO, and show a good agreement with the July NAO pattern presented by *Barnston* *and Livezey* [1987]. The major action center covers a large part of Europe (Figures 3a, c), and along with the respective pattern of July precipitation (Figure 1e), suggests that an anti-cyclonic (cyclonic) anomaly results in deficient (excessive) precipitation over a large portion of Europe. The PCs of this mode (not shown) are strongly correlated to the July NAO index (0.73 and 0.49 for SLP and 500hPa respectively) and to PCs of the EOF-1 of July precipitation (0.85 and 0.91 for SLP and 500hPa).

In July the spatial patterns of the EOF-2 of 500hPa and SLP (Figures 3b, d) are characterized by two dominating action centers located over the northeastern North Atlantic and over European Russia. Minor action centers of opposite polarity over Scandinavia, Greenland and western North Atlantic are seen in the EOF-2 pattern for SLP (Figure 3d). Structurally the obtained EOF-2 patterns are similar to the EAWR pattern obtained by *Barnston and Livezey* [1987] and referred to as the Eurasia-2 pattern in their study. Respective PCs are significantly correlated to the July EAWR index (0.74 and 0.72 for SLP and 500hPa respectively), but not correlated to PCs of the second EOF mode of July precipitation because latter, as shown above, is associated with the Scandinavian teleconnection.

Summarizing results of this section, we note that during summer the first EOF mode of European precipitation is stable (in terms of its month-to-month variations) and is strongly linked to the major regional climate signal – the NAO. The second EOF mode of regional precipitation is less stable and demonstrates some structural changes during the summer season. Our results suggest that the major driver for this mode is the SCA teleconnection pattern [*Barnston and Livezey,* 1987], which is not among the leading modes of the regional atmospheric circulation during summer season.

4. Links between European precipitation and regional evaporation

In this section we examine links between European precipitation and evaporation in four regions that can potentially impact variability of European precipitation during the warm season. These regions are the North Atlantic Ocean, the Baltic and Mediterranean Seas, and Europe (i.e., European land surface). We first reveal the leading modes of evaporation in each region by applying EOF analysis to detrended time series of evaporation from the WHOI dataset (for oceanic/marine regions) and from the NCEP/NCAR reanalysis (for European land surface) for 1979-2006. Spatial patterns of the first and second EOF modes of evaporation for the Baltic Sea, Mediterranean Sea and Europe are shown respectively in Figures 5-7. Note, the spatial patterns obtained for other summer months are similar to those presented in Figures 5-7. Further, we analyze links between leading EOF modes of evaporation in aforementioned regions and leading modes of precipitation over Europe. Since we did not find statistically significant links between large-scale European precipitation variability and evaporation in the North Atlantic during summer, we exclude this region from our further analysis. Note, however, that local precipitation variability in some European regions (e.g., northern Scandinavia) can be influenced by the North Atlantic moisture transport.

Since our analysis of the leading modes of precipitation and evaporation (and their relationships) characterize variations of some fractions of total precipitation (or evaporation), it is of interest first to look and compare lump precipitation/evaporation in the regions of interest and their interannual variations. For July, the mean total water flux (and its standard deviation, both in km^3/day) is 19.3 (2.85) for European precipitation, 31.2 (1.60) for European evaporation, 8.16 (1.02) for Mediterranean evaporation, and 1.51 (0.31) for the Baltic Sea evaporation. Thus, it is evident that the major players for the regional hydrological cycle are the European land area and the Mediterranean Sea. Figure 4 depicts anomalies of the total water flux estimated for European precipitation and evaporation, and for evaporation from the Mediterranean/Black Seas and Baltic/North Seas. Correspondence between the presented time series is obvious. Correlation between European precipitation and evaporation is 0.53. When Mediterranean evaporation is added to European evaporation, correlation with precipitation increases to 0.58. Adding of Baltic/North Sea evaporation does not affect significantly correlation with European precipitation (0.57). This suggests that Mediterranean evaporation may explain a significant portion of European precipitation variance, however the role of local (i.e. from European land surface) evaporation is likely to be most important. We note that these (rather rough) estimates just provide useful background for our further analysis, whereas accurate balance estimates for regional hydrological cycle are beyond the scope of the present study.

We extended slightly the domain of analysis for the Baltic Sea region since both the North Sea and Baltic Sea are influenced by the same atmospheric circulation patterns (Figure 3), and because the amount of grid points covering the Baltic Sea is relatively low. In July the first EOF mode of evaporation in the extended Baltic/North Sea region explains about half (51.9%) of its total variability. Its spatial pattern reflects coherent variations of evaporation over the entire domain of analysis (Figure 5a). Although there is significant correlation to PC-1 of precipitation in August, in general principal components (not shown) of this mode do not demonstrate significant correlations to PC-1 and PC-2 of precipitation (Table 2), suggesting that this mode does not affect significantly large-scale variability of European precipitation during summer. The second EOF mode of evaporation in the Baltic/North Sea region accounts for 18.7% of its total variability in July. Its spatial pattern depicts a dipole with opposite variations of evaporation in the Baltic Sea and the North Sea (Figure 5b). Such a pattern presumably reflects more local (compared to the first EOF mode) forcings of the regional evaporation variability. Principal components of this mode (not shown) demonstrate significant correlation to the EOF-1 of European precipitation in June and July, and to the EOF-2 in August (Table 2), suggesting an influence of this mode on variability of regional precipitation. However, since the EOF-2 explains a relatively low fraction of the total evaporation, we presume that this influence is not large.

The first EOF mode of evaporation from the surface of the Mediterranean Sea in July explains 45.6% of its total variability. The spatial pattern of this mode is characterized by coherent variations of evaporation over the entire Mediterranean Sea (Figure 6a). Principal components (not shown) of this mode correlate significantly to PC-1 of precipitation over Europe (Table 2), suggesting an essential influence of this mode on summertime variability of regional precipitation. More specifically, Figures 1e and 6a indicate that below (above) normal precipitation over a large part of Europe is associated with decreased (increased) evaporation from the surface of the Mediterranean Sea. Dynamical background for this association (Figure 3c) suggests that the positive (negative) phase of the summer NAO leads to reduced (enhanced) advection of the Mediterranean moisture into eastern Europe and European Russia, resulting in below (above) normal precipitation in these regions. Note, however, that in June and August the first EOF mode of Mediterranean evaporation is associated with the second EOF of European precipitation (Table 2). The EOF-2 accounts for 21.3% of total variability of evaporation in the Mediterranean Sea in July. Its spatial pattern is characterized by the zonal dipole with opposite variations of evaporation in the western and eastern parts of the sea (Figure 6b). Principal components of the EOF-2 (not shown) demonstrate significant correlation to the EOF-1 of European precipitation in July and August (Table 2). Thus, our results suggest that both the first and the second EOF modes, explaining together about 67% of total variability of Mediterranean evaporation, affect summertime variability of precipitation over Europe. Although aforementioned correlations are almost equal, the influence of the first EOF mode is indeed significantly larger since it explains double the fraction of the total variability of evaporation.

The spatial pattern of the EOF-1 of evaporation from the European land surface is characterized by the major action center covering almost all of Europe from the Iberian Peninsula and France to Scandinavia and European Russia where the largest loadings are revealed (Figure 7a). A minor action center of opposite polarity is revealed over the Balkans and eastern Mediterranean – Black Sea region. This mode explains 24.9% of the total variability of regional evaporation. Principal components of this mode show high correlations to the PC-1 of European precipitation in June, July and August (Table 2) implying coupling of the leading modes of European precipitation and evaporation during the warm season. Above detected high correlations (the largest among those considered in our analysis, see Table 2), however, does not point to causal relationships between regional precipitation and land surface evaporation, and may indicate a positive feedback when enhanced precipitation results in increased soil moisture and evaporation, which amplifies regional precipitation. In this regard, it is of interest to compare amounts of precipitation and evaporation and magnitudes of their interannual variability. Over central/eastern Europe and European Russia (i.e. regions of the largest variability of the summer precipitation, see Figure 1e) July precipitation values (not shown) vary from 2.5 mm/day to 3.5 mm/day, whereas reanalysis evaporation in this region varies in the range 3.5 - 4.5 mm/day, thus exceeding regional precipitation. On the other hand standard deviations (not shown) of precipitation (1.0 -1.4 mm/day) in the region are approximately twice those of evaporation (0.4 – 0.7 mm/day). Values of evaporation and its standard deviations in the Mediterranean Sea are comparable to those over land. The largest July evaporation (reaching 3.6 mm/day) is observed in the eastern Mediterranean Sea. Overall, this suggest, that both precipitation and local evaporation may affect each other. Although the magnitudes of interannual variability of evaporation are smaller than those of precipitation, they are evidently non-negligible (see also Figure 4). The second EOF mode of evaporation from the European land surface in July explains only 12.8% of its total variability. Its spatial pattern represents a meridional dipole with opposite variations of evaporation north/south off approximately 53°-55°N latitude (Figure 7b). Only in August principal components of this mode significantly correlated to the second EOF mode of regional precipitation (Table 2).

To summarize results of this section, we note that our analysis suggests that, in contrast to the winter season, during summer the evaporation in the North Atlantic does not affect continental-scale interannual variability of precipitation over Europe. However, smaller scale variability of precipitation, particularly in some coastal regions, can be significantly affected by this factor [e.g., *Lenderink et al.,* 2009]. Our analysis indicates a significant role of land surface evaporation in the variability of European precipitation during the warm season. This result supports recent findings based on model simulations [*Koster and Suarez,* 1995; *Schär et al.,* 1999; *Seneviratne et al.,* 2006]. Note, however, that in contrast to the North Atlantic, Baltic and Mediterranean Seas where observation-based data were used, for the land surface we used evaporation from reanalysis products with well known limitations. We also found statistically significant links between evaporation in the Baltic and Mediterranean Seas and interannual variability of precipitation over Europe. However, we believe that the major regions affecting (through evaporation) regional precipitation during the warm season are the European land area and the Mediterranean Sea, while evaporation in the Baltic Sea plays a minor role. Overall, results of this section suggest that in contrast to the winter season when moisture advection from the North Atlantic into the European region plays a dominant role in regional precipitation variability, during boreal summer local processes make significant contribution to the interannual variability of European precipitation.

5. Summary and discussion

In the present study we analyzed the leading modes of interannual variability of summertime precipitation over Europe based on the data from the GPCP dataset for 1979-2006 [*Huffman et al.,* 1997; *Adler et al.,* 2003]. We also investigated the relation of these modes to regional atmospheric circulation, and their links to evaporation in the North Atlantic Ocean, Baltic and Mediterranean Seas, as well as to evaporation from the European land surface.

It is shown that the first EOF mode of European precipitation is rather stable (in terms of its spatial-temporal structure) during the summer season, and is characterized by a tripole-like pattern with large coherent variations over a wide region extending from the British Isles to European Russia. Relatively weak precipitation variations of opposite sign are revealed north and south of the above region. This mode is associated with the summer NAO [*e.g., Zveryaev,* 2004; *Folland et al.,* 2009]. Since anomalies in atmospheric circulation during summer are not as large as during winter, and because precipitation is one of the most variable climate parameters, it is not obvious to expect the revealed stability of the first mode of summer precipitation. For the first time we show that during recent decades the second EOF mode of summer precipitation (characterized by meridional dipole structure) is less stable, and is linked to the Scandinavian teleconnection [*Barnston and Livezey,* 1987]. Note, analysis performed for the century-long time series of precipitation [*Zveryaev,* 2006] did not reveal such a link. Moreover, it was shown that different mechanisms can be major drivers for European precipitation variability during different climate periods [*Zveryaev,* 2006; 2009]. In particular, it was demonstrated that during periods of weak NAO influence on European precipitation, the Scandinavian teleconnection played a role of major driver for regional precipitation variability in spring and fall [*Zveryaev,* 2009]. Therefore, our findings characterize the most recent climate period which is recognized as the warmest period in the history of instrumental observations. Also, it should be emphasized that the first two EOF modes considered in the present study describe together up to 35% of total variability of European precipitation. Thus, a substantial portion of summertime precipitation variability over Europe remains undescribed, and mechanisms that drive this part of precipitation variability are not clear, implying necessity of further studies in this direction. It is clear that present study based on the analysis of monthly data has certain limitations in investigation of such mechanisms. In this regard an analysis of summertime precipitation variability at shorter (e.g., synoptic, sub-synoptic, etc.) time scales based on data having higher temporal resolution looks very promising and can potentially shed more light on the mechanisms driving regional precipitation variability.

Analysis of links between European precipitation and evaporation has shown that, in contrast to the winter season, when regional precipitation variability is mostly determined by the NAO-driven moisture advection from the North Atlantic, summertime continental scale variability of precipitation is not associated with evaporation in the North Atlantic. On the contrary, our results suggest a significant role of the local processes, in particular land surface evaporation, in variability of regional precipitation during the warm season, supporting recent model-based results [*e.g., Schär et al.,* 1999; *Seneviratne et al.,* 2006]. Because we used in our study reanalysis data having well known limitations, further analysis of the role of land surface evaporation in interannual variability of European precipitation during the warm season is needed. In particular an analysis (based on higher temporal and spatial resolution data) of the relative roles of the local evaporation and regimes of regional atmospheric circulation focused on different time scales would be of great interest since these roles can vary significantly depending on time scales. It should be noted that a revealed links between the leading modes of regional precipitation and land surface evaporation does not indicate causal relationships between these variables, and may reflect a positive feedback when enhanced precipitation leads to an increase of soil moisture and evaporation, which in turn amplifies regional precipitation. Thus, to get deeper insight into causal relationships between European precipitation and land surface evaporation, model experiments are highly desirable. For example, simulations of European climate with high-resolution regional climate models [e.g., Vidale et al., 2003, 2007] look very promising. Although there is considerable spread in the models' ability to represent the observed summer climate variability, we believe that further experiments, for instance applying climatological ancilliary fields to restrict the variability of surface moisture fluxes and analyzing the dependence of model precipitation on such forcings, could provide informative results and make causal relationships in the regional hydrological cycle clearer.

We also found significant links between summertime European precipitation and evaporation in the Mediterranean Sea which also (along with the land surface) can be viewed as a local (rather than remote) source of moisture. It seems that the influence of the Baltic Sea evaporation on regional precipitation is not large (although statistically significant links are detected) and probably limited to the Baltic region.

The present study highlights mechanisms driving summertime interannual variability of precipitation over Europe. Since the summertime NAO is structurally different from that for other seasons, its impact on summer precipitation variability over Europe is also principally different. We found that during summer the leading modes of regional precipitation are not associated with evaporation in the North Atlantic, but linked to local processes such as evaporation from the European land surface and from the surface of the Mediterranean Sea. However, since our assessment of the links to land surface evaporation is limited to reanalysis products, we hope that further diagnostic studies of the observational data as well as model experiments will allow obtaining more accurate estimates of these links.

Acknowledgments

This research was supported by the Royal Society grant (International Incoming Short Visits, IV0866722). A major part of the present study has been performed during IIZ work at the Environmental Systems Science Centre, University of Reading as a visiting scientist. IIZ was also supported by the Russian Ministry of Education and Science under the Federal Focal Program "World Ocean" (contract No. 01.420.1.2.0001) and Russian Academy of Sciences Research Program "Fundamental problems of Oceanology". Discussions with Dr. Sergey Gulev are appreciated. The NCEP data was extracted from NOAA-CIRES Climate Diagnostics Center. The manuscript was significantly improved by the constructive comments of three anonymous reviewers.

References

Adler, R.F., and coauthors (2003), The Version-2 Global Precipitation Climatology Project (GPCP) monthly precipitation analysis (1979-present), *J. Hydromet.,* 4, 1147-1167.

Barnston, A.G., and R.E. Livezey (1987), Classification, seasonality and persistence of low-frequency atmospheric circulation patterns, *Mon. Weather Rev.,* 115, 1083-1126.

Bendat, J.S., and A.G. Piersol (1966), *Measurement and Analysis of Random Data*, 390 pp., John Wiley, Hoboken, N. J.

Blackburn, M., J. Methven, and N. Roberts (2008), Large-scale context for the UK floods in summer 2007, *Weather,* 63, 280-288.

Casty, C., C.C. Raible, T.F. Stocker, H. Wanner, and J. Luterbacher (2007), A European pattern climatology 1766-2000. *Clim. Dyn.,* doi: 10.1007/s00382-007-0257-6.

Christensen, J.H., and O.B. Christensen (2003), Severe summertime flooding in Europe, *Nature,* 421, 805-806.

Colman, A., and M. Davey (1999), Prediction of summer temperature, rainfall and pressure in Europe from preceding winter North Atlantic ocean temperature, *Int. J. Climatol.,* 19, 513-536.

Dirmeyer, P.A., M.J. Fennessy, and L. Marx (2003), Low skill in dynamical prediction of boreal summer climate: Grounds for looking beyond sea surface temperature, *J. Climate,* 16, 995-1002.

Folland, C.K., J. Knight, H.W. Linderholm, D. Fereday, S. Ineson, and J.W. Hurrell (2009), The Summer North Atlantic Oscillation: Past, Present, and Future, *J. Climate,* 22, 1082-1103.

Huffman, G.J., and coauthors (1997), The Global Precipitation Climatology Project (GPCP) combined precipitation dataset, *Bull. Amer. Meteorol. Soc.,* 78, 5-20.

Hurrell, J.W. (1995), Decadal trends in the North Atlantic oscillation: Regional temperature and precipitation, *Science,* 269, 676-679.

Hurrell, J.W., and C.K. Folland (2002), A change in the summer atmospheric circulation over the North Atlantic, *CLIVAR Exch.,* 7(3-4), 52-54.

Kalnay, E., Kanamitsu, M., Kistler, R., Collins, W., Deaven, D., Gandin, L., Iredell, M., Saha, S., White, G., Wollen, J., Zhu, Y., Chelliah, M., Ebisuzaki, W., Higgins, W., Janowiak, J., Mo, K. C., Ropelewski, C., Wang, J., Leetma, A., Reynolds, R., Jenne, R. and D. Joseph (1996), The NCEP/NCAR 40-year reanalysis Project. *Bull. Amer. Met. Soc.,* 77, No. 3, 437-471.

Koenigk, T., and U. Mikolajewicz (2008), Seasonal to interannual climate predictability in mid and high northern latitudes in a global climate model, *Clim. Dyn.,* 28, doi:10.1007/s00382-008-0419-1.

Koster, R.D., and M.J. Suarez (1995), Relative contributions of land and ocean processes to precipitation variability, *J. Geophys. Res.,* 100, D7, 13775-13790.

Koster, R.D., and coauthors (2004), Regions of strong coupling between soil moisture and precipitation, *Science,* 305, 1138-1140.

Lenderink, G., E. van Meijgaard, and F. Selten (2009), Intense coastal rainfall in the Netherlands in response to high sea surface temperatures: analysis of the event of August 2006 from the perspective of a changing climate, *Clim. Dyn.,* 32, 19-33.

Mächel H., A. Kapala, and H. Flohn (1998), Behaviour of the centres of action above the Atlantic since 1881. Part I: Characteristics of seasonal and interannual variability, *Int. J. Climatol.,* 18, 1-22.

Marsh, T. J. and J. Hannaford (2007), The summer 2007 floods in England and Wales - a hydrological appraisal. Centre for Ecology & Hydrology. 32pp.

Mitchell, T.D., and P.D. Jones (2005), An improved method of constructing a database of monthly climate observations and associated high-resolution grids, *Int. J. Climatol.,* 25, 693-712.

New, M.G., M. Hulme, and P.D. Jones (1999), Representing twentieth-century space-time climate variability. Part I: Development of a 1961-90 mean monthly terrestrial climatology, *J. Climate,* 12, 829-856.

North, G.R., T.L. Bell, and R.F. Calahan (1982), Sampling errors in the estimation of empirical orthogonal functions, *Mon. Wea. Rev.,* 110, 699-706.

Ogi, M., K. Yamazaki, and Y. Tachibana (2005), The summer northern annular mode and abnormal summer weather in 2003, *Geophys. Res. Lett.,* 32, L04706.

Pal, J.S., F. Giorgi, and X. Bi (2004), Consistency of recent European summer precipitation trends and extremes with future regional climate projections, *Geophys. Res. Lett.,* 31, L13202.

Portis, D.H., J.E. Walsh, M. El Hamly, and P.J. Lamb (2001), Seasonality of the North Atlantic Oscillation, *J. Clim.,* 14, 2069-2078.

Qian, B., H. Xu, and J. Corte-Real (2000), Spatial-temporal structures of quasi-periodic oscillations in precipitation over Europe, *Int. J. Climatol.,* 20, 1583-1598.

Roads, J.O., S.-C. Chen, M. Kanamitsu, and H. Juang (1999), Surface water characteristics in NCEP global spectral model and reanalysis, *J. Geophys. Res.,* 104, D16, 19307-19327.

Seneviratne, S.I., D. Lüthi, M. Litschi, and C. Schär (2006), Land-atmosphere coupling and climate change in Europe, *Nature,* 443, 205-209.

Schär, C., D. Lüthi, and U. Beyerle (1999), The soil-precipitation feedback: a process study with a regional climate model, *J. Climate,* 12, 722-741.

Schär, C., D. Lüthi, and U. Beyerle (2004), The role of increasing temperature variability in European summer heatwaves, *Nature,* 427, 332-336.

Trenberth, K.E. (1999), Atmospheric moisture recycling: Role of advection and local evaporation, *J. Climate,* 12, 1368-1381.

Trenberth, K.E., P.D. Jones, P. Ambenje, R. Bojariu, D. Easterling, A. Klein Tank, D. Parker, F. Rahimzadeh, J.A. Renwick, M. Rusticucci, B. Soden and P. Zhai (2007), Observations: Surface and Atmospheric Climate Change. In: *Climate Change 2007: The Physical Science Basis*. Contribution of Working Group I to the Fourth Assessment Report of the Intergovernmental Panel on Climate Change [Solomon, S., D. Qin, M. Manning, Z. Chen, M. Marquis, K.B. Averyt, M. Tignor and H.L. Miller (eds.)]. Cambridge University Press, Cambridge, United Kingdom and New York, NY, USA.

Vidale P.L., D. Lüthi, C. Frei, S.I. Seneviratne, and C. Schär (2003), Predictability and uncertainty in a regional climate model, *J. Geophys. Res.,* 108 (D18): 4586, doi: 10.1029/2002JD002810.

Vidale P.L., D. Lüthi, R. Wegmann, and C. Schär (2007), European climate variability in a heterogeneous multi-model ensemble, *Clim. Change,* doi: 10.1007/s10584-006-9218-z.

von Storch, H., and A. Navarra (1995), *Analysis of Climate Variability*, 334 pp., Springer-Verlag, New-York.

Wanner, H., R. Rickli, E. Salvisber, C. Schmutz and M. Schuepp (1997), Global climate change and variability and its influence on Alpine climate – concepts and observations. *Theor. Appl. Climatol.,* 58, 221-243.

Wilks, D.S. (1995), *Statistical Methods in the Atmospheric Sciences*, 467 pp., Academic, San Diego, Calif.

Yu, L., and R.A. Weller (2007), Objectively analyzed air-sea heat fluxes for the global ice-free oceans (1981-2005), *Bull. Amer. Meteorol. Soc.,* 88, 527-539.

Yu, L., R.A. Weller, and B. Sun (2004), Improving latent and sensible heat flux estimates for the Atlantic Ocean (1988-99) by a synthesis approach, *J. Climate,* 17**,** 373-393.

Zolina, O., A. Kapala, C. Simmer, and S. Gulev (2004), Analysis of extreme precipitation over Europe from different reanalysis: a comparative assessment. *Global and Planetary Change,* 44, 129-161.

Zolina, O., C. Simmer, A. Kapala, S. Bachner, S. K. Gulev, and H. Maechel, (2008), Seasonally dependent changes of precipitation extremes over Germany since 1950 from a very dense observational network, *J. Geophys. Res.,* 113, D06110, doi:10.1029/2007JD008393.

Zveryaev, I.I. (2004), Seasonality in precipitation variability over Europe, *J. Geophys. Res.,* 109, D05103, doi: 10.1029/2003JD003668.

Zveryaev, I.I. (2006), Seasonally varying modes in long-term variability of European precipitation during the 20th century, *J. Geophys. Res.,* 111, D21116, doi: 10.1029/2005JD006821.

Zveryaev, I.I. (2009), Interdecadal changes in the links between European precipitation and atmospheric circulation during boreal spring and fall. *Tellus,* 61, doi: 10.1111/j.1600-0870.2008.00360.x.

Table Captions

Table 1. Correlation coefficients between PC-1 and PC-2 of summer, June, July and August precipitation, and indices of teleconnection patterns. Coefficients, shown in bold, are statistically significant at the 95% significance level.

Table 2. Correlation coefficients between PC-1 and PC-2 of June, July and August precipitation, and evaporation in different regions. Coefficients, shown in bold, are statistically significant at the 95% significance level.

Figure Captions

Figure 1. Spatial patterns (mm/day) of the first two EOF modes of the summer mean (a, b), June (c, d), July (e, f) and August (g, h) GPCP precipitation (1979-2006). Red (blue) color indicates positive (negative) values.

Figure 2. Principal components of the first two EOF modes of the summer mean (a, b), June (c, d), July (e, f) and August (g, h) GPCP precipitation (1979-2006). Blue (green) curves depict the NAO (SCA) index.

Figure 3. Spatial patterns of the first two EOF modes of July 500hPa (a, b, in meters) and SLP (c, d, in millibars) fields (1979-2006). Red (blue) color indicates positive (negative) values.

Figure 4. Total water flux anomalies (in km^3/day) for July estimated for different regions.

Figure 5. Spatial patterns (mm/day) of the first two EOF modes of July evaporation in the Baltic Sea – North Sea region (1979-2006). Red (blue) color indicates positive (negative) values.

Figure 6. Spatial patterns (mm/day) of the first two EOF modes of July evaporation from the surface of Mediterranean Sea (1979-2006). Red (blue) color indicates positive (negative) values.

Figure 7. Spatial patterns (mm/day) of the first two EOF modes of July evaporation from the European land surface (1979-2006). Red (blue) color indicates positive (negative) values.

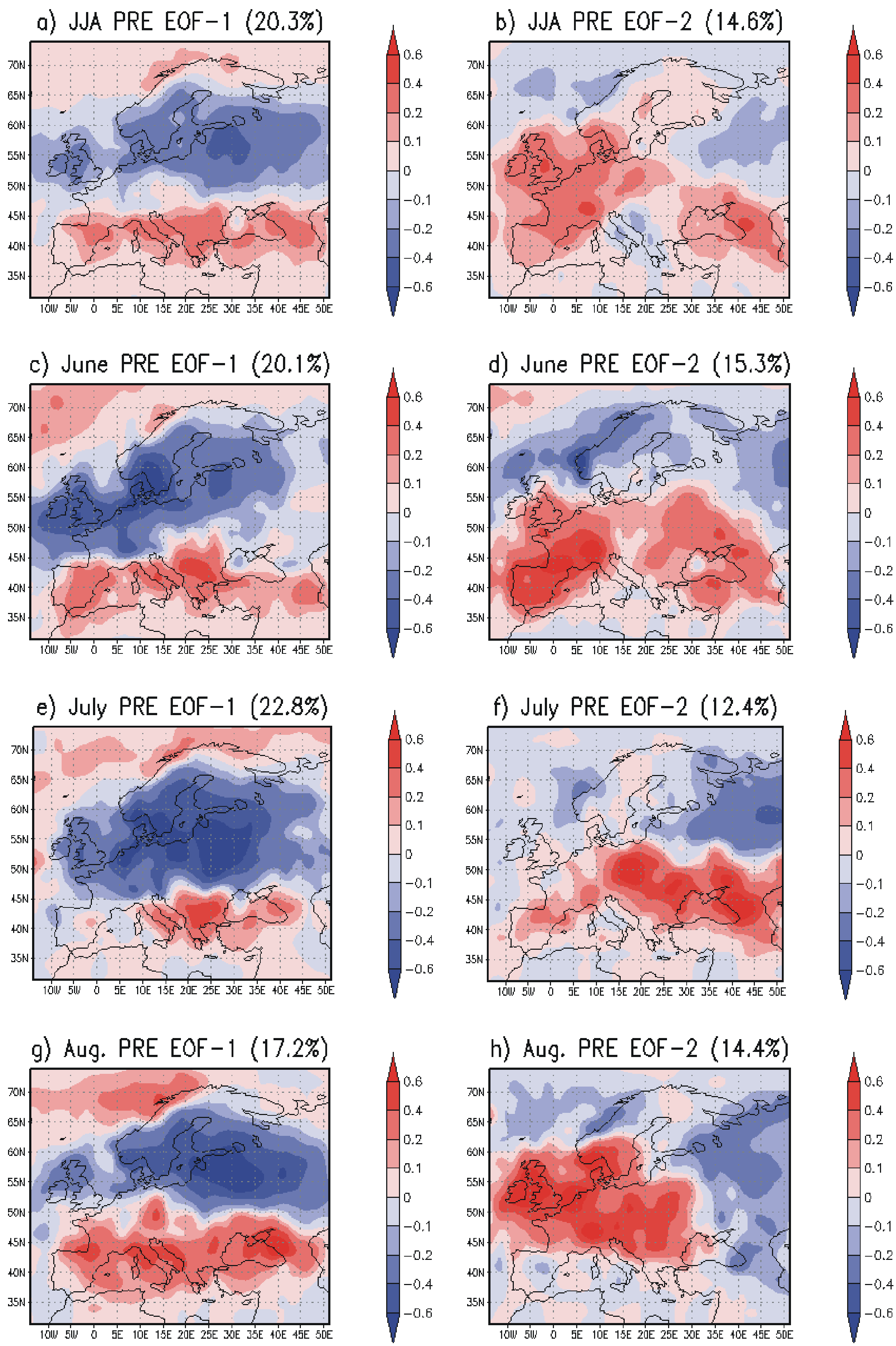
a) JJA PRE EOF-1 (20.3%)
b) JJA PRE EOF-2 (14.6%)
c) June PRE EOF-1 (20.1%)
d) June PRE EOF-2 (15.3%)
e) July PRE EOF-1 (22.8%)
f) July PRE EOF-2 (12.4%)
g) Aug. PRE EOF-1 (17.2%)
h) Aug. PRE EOF-2 (14.4%)
70N
65N
60N
55N
50N
45N
40N
35N
10W 5W 0 5E 10E 15E 20E 25E 30E 35E 40E 45E 50E
0.6
0.4
0.2
0.1
0
−0.1
−0.2
−0.4
−0.6

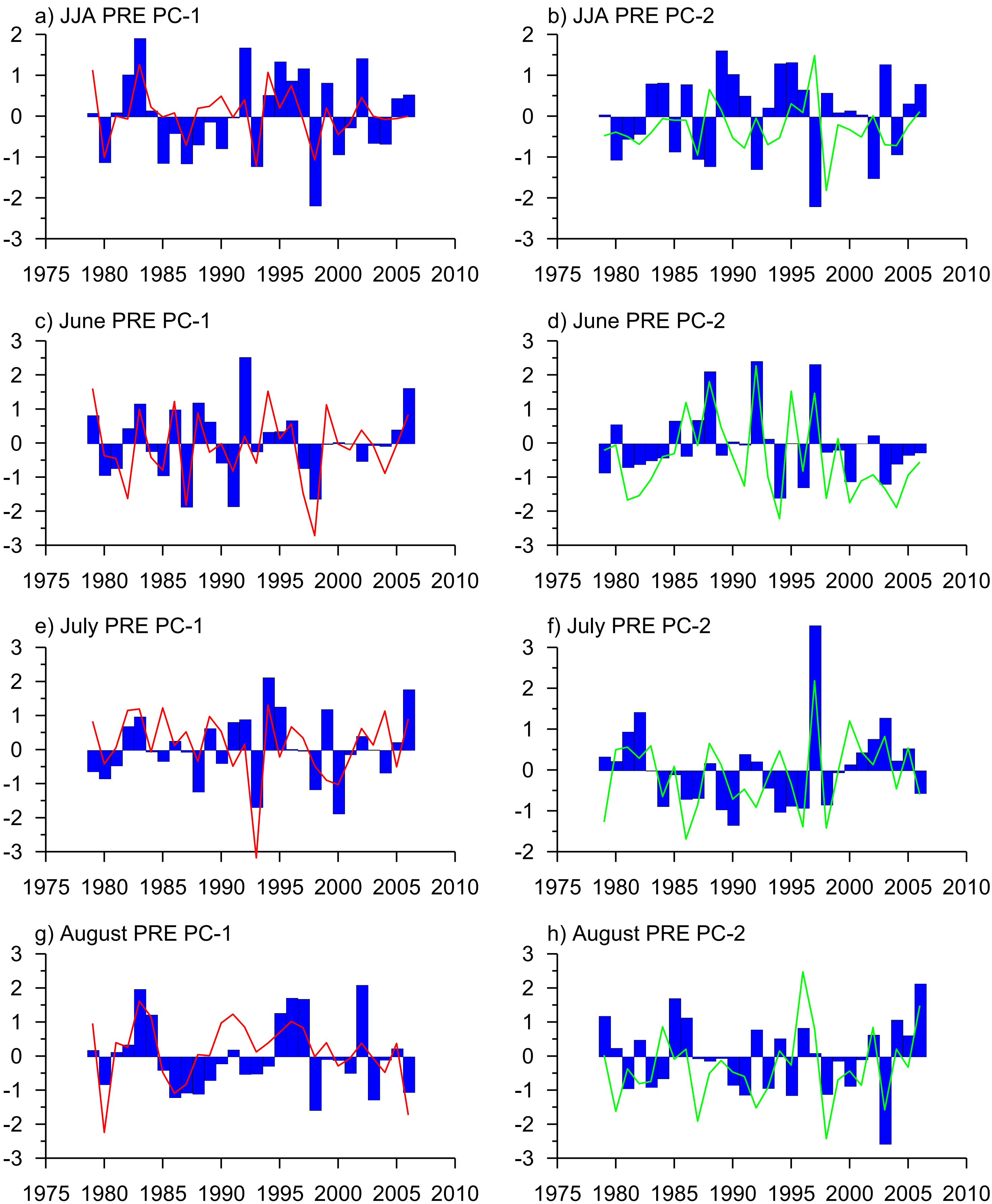

a) JJA PRE PC-1
b) JJA PRE PC-2
c) June PRE PC-1
d) June PRE PC-2
e) July PRE PC-1
f) July PRE PC-2
g) August PRE PC-1
h) August PRE PC-2
1975 1980 1985 1990 1995 2000 2005 2010

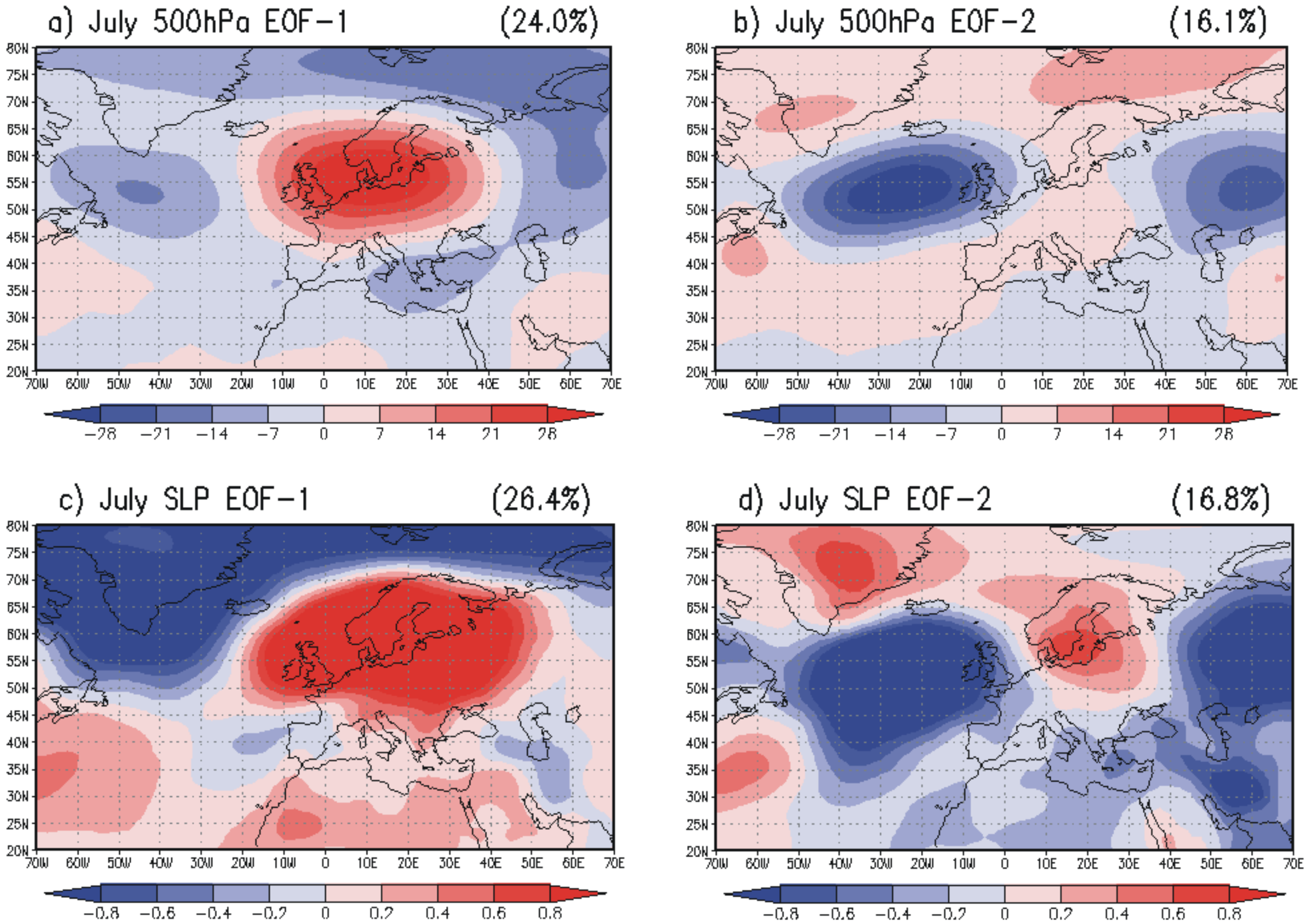
a) July 500hPa EOF-1
(24.0%)
b) July 500hPa EOF-2
(16.1%)
−28 −21 −14 −7 0 7 14 21 28
c) July SLP EOF-1
(26.4%)
d) July SLP EOF-2
(16.8%)
−0.8 −0.6 −0.4 −0.2 0 0.2 0.4 0.6 0.8
20N 25N 30N 35N 40N 45N 50N 55N 60N 65N 70N 75N 80N
70W 60W 50W 40W 30W 20W 10W 0 10E 20E 30E 40E 50E 60E 70E

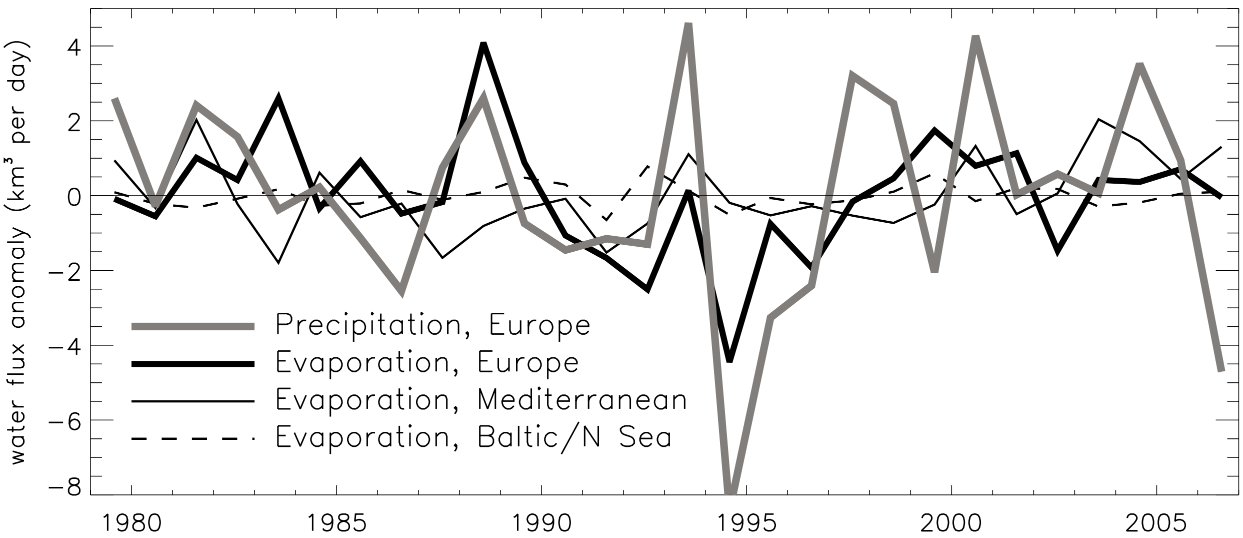

water flux anomaly (km³ per day)
Precipitation, Europe
Evaporation, Europe
Evaporation, Mediterranean
Evaporation, Baltic/N Sea
4
2
0
−2
−4
−6
−8
1980
1985
1990
1995
2000
2005

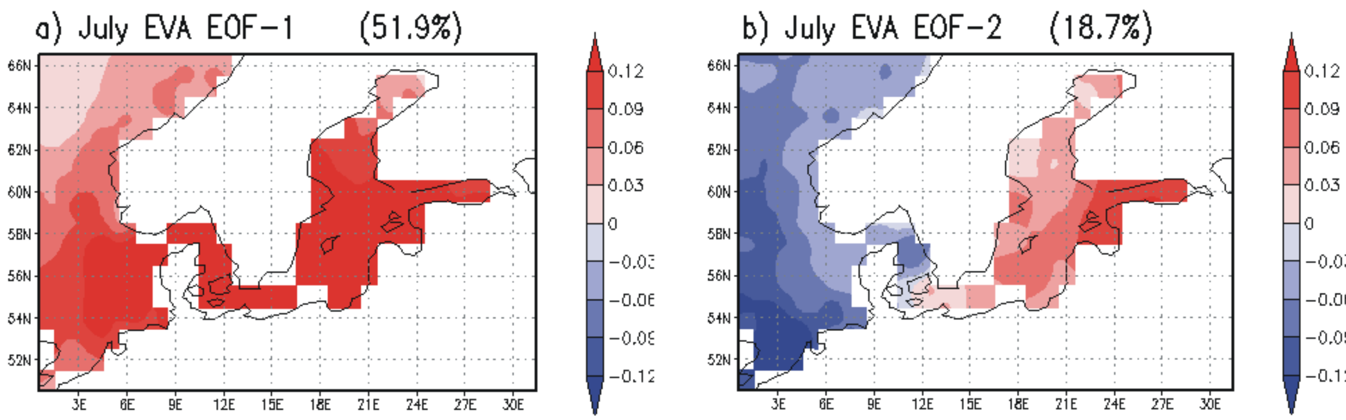

a) July EVA EOF-1 (51.9%)
b) July EVA EOF-2 (18.7%)
66N
64N
62N
60N
58N
56N
54N
52N
3E
6E
9E
12E
15E
18E
21E
24E
27E
30E
0.12
0.09
0.06
0.03
0

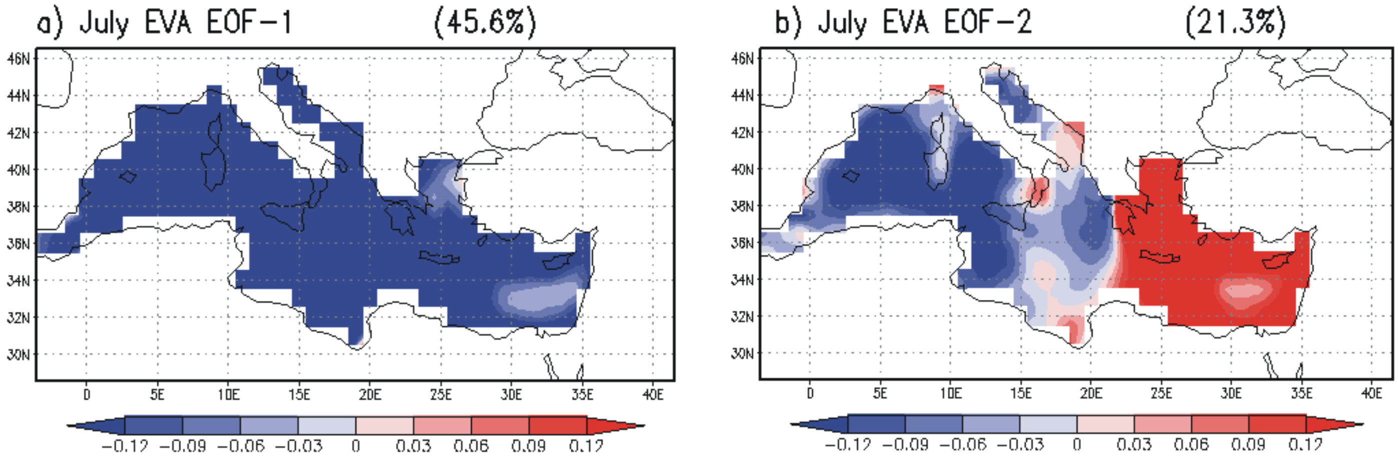
a) July EVA EOF-1 (45.6%)
b) July EVA EOF-2 (21.3%)
46N
44N
42N
40N
38N
36N
34N
32N
30N
0
5E
10E
15E
20E
25E
30E
35E
40E
−0.12 −0.09 −0.06 −0.03 0 0.03 0.06 0.09 0.12

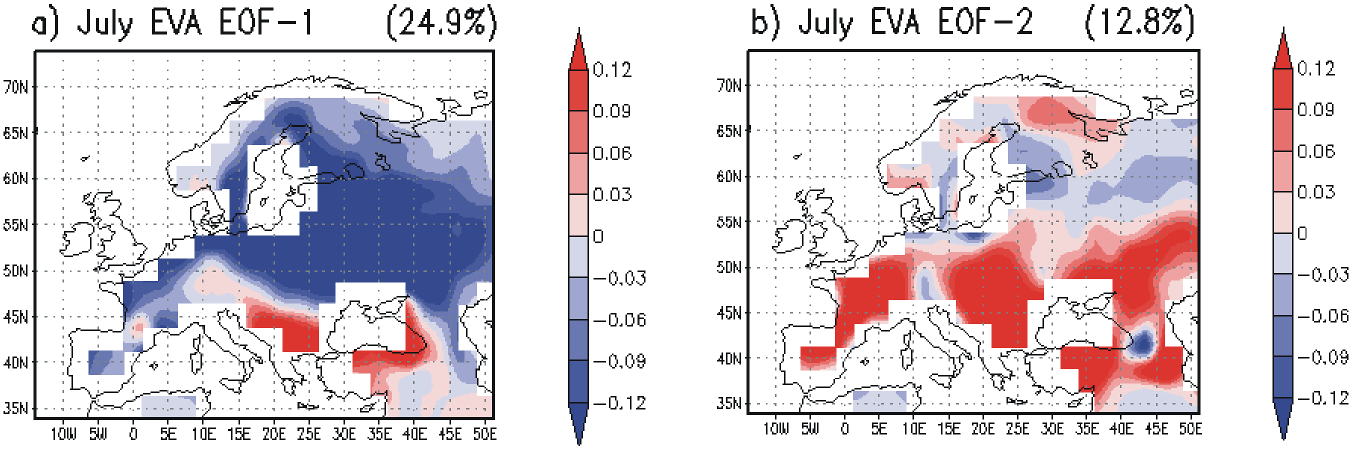
a) July EVA EOF-1 (24.9%)
b) July EVA EOF-2 (12.8%)
70N
65N
60N
55N
50N
45N
40N
35N
10W 5W 0 5E 10E 15E 20E 25E 30E 35E 40E 45E 50E
0.12
0.09
0.06
0.03
0
−0.03
−0.06
−0.09
−0.12

Table 1. Correlation coefficients between PC-1 and PC-2 of summer, June, July and August precipitation, and indices of teleconnection patterns. Coefficients, shown in bold, are statistically significant at the 95% significance level.

	Summer		**June**		**July**		**August**	
	PC-1	PC-2	PC-1	PC-2	PC-1	PC-2	PC-1	PC-2
NAO	**0.67**	0.14	**0.68**	0.48	**0.50**	-0.12	**0.63**	0.04
SCA	0.10	0.30	-0.16	**0.76**	-0.21	**0.65**	-0.26	**0.49**

Table 2. Correlation coefficients between PC-1 and PC-2 of June, July and August precipitation, and evaporation in different regions. Coefficients, shown in bold, are statistically significant at the 95% significance level.

Europe Precip.	**N. Atlantic**		**Baltic**		**Mediterranean**		**Europe**	
	EVA1	EVA2	EVA1	EVA2	EVA1	EVA2	EVA1	EVA2
PRE1(Jun)	-0.03	***	-0.10	**0.47**	0.31	0.01	**0.64**	0.05
PRE2(Jun)	0.33	***	0.02	0.12	**0.51**	0.21	0.13	0.29
PRE1(Jul)	-0.14	***	0.04	**0.48**	**0.43**	**-0.42**	**0.78**	0.34
PRE2(Jul)	-0.10	***	-0.16	0.17	-0.21	0.23	-0.26	0.30
PRE1(Aug)	-0.35	***	**0.43**	-0.28	-0.03	**-0.44**	**0.62**	0.20
PRE2(Aug)	0.20	***	0.26	**0.50**	**0.49**	0.22	0.10	**0.59**